Clinical Use of Cerebrovascular Compliance Imaging to Evaluate Revascularization in Patients With Moyamoya

Jennifer M. Watchmaker, PhD[*]
Blaise deB. Frederick, PhD[‡§]
Matthew R. Fusco, MD[¶]
Larry T. Davis, MD[‖]
Meher R. Juttukonda, PhD[*]
Sarah K. Lants, BA[*]
Howard S. Kirshner, MD[#]
Manus J. Donahue, PhD[*#**]

[*]Vanderbilt University of Institute of Imaging Science, Vanderbilt University Medical Center, Nashville, Tennessee; [‡]Brain Imaging Center, McLean Hospital, Belmont, Massachusetts; [§]Consolidated Department of Psychiatry, Harvard Medical School, Boston Massachusetts; [¶]Department of Neurological Surgery, Vanderbilt University Medical Center, Nashville, Tennessee; [‖]Department of Radiology and Radiological Sciences, Vanderbilt University Medical Center, Nashville, Tennessee; [#]Department of Neurology, Vanderbilt University Medical Center, Nashville, Tennessee; [**]Department of Psychiatry, Vanderbilt University Medical Center, Nashville, Tennessee

Correspondence:
Manus J. Donahue, PhD,
Vanderbilt University Institute of Imaging Science,
1161 21st Avenue South,
Nashville, TN 37232.
E-mail: mjd@alumni.duke.edu

Received, June 9, 2017.
Accepted, December 18, 2017.
Published Online, March 8, 2018.

BACKGROUND: Surgical revascularization is often performed in patients with moyamoya, however routine tools for efficacy evaluation are underdeveloped. The gold standard is digital subtraction angiography (DSA); however, DSA requires ionizing radiation and procedural risk, and therefore is suboptimal for routine surveillance of parenchymal health.

OBJECTIVE: To determine whether parenchymal vascular compliance measures, obtained noninvasively using magnetic resonance imaging (MRI), provide surrogates to revascularization success by comparing measures with DSA before and after surgical revascularization.

METHODS: Twenty surgical hemispheres with DSA and MRI performed before and after revascularization were evaluated. Cerebrovascular reactivity (CVR)-weighted images were acquired using hypercapnic 3-Tesla gradient echo blood oxygenation level-dependent MRI. Standard and novel analysis algorithms were applied (i) to quantify relative CVR ($rCVR_{RAW}$), and decompose this response into (ii) relative maximum CVR ($rCVR_{MAX}$) and (iii) a surrogate measure of the time for parenchyma to respond maximally to the stimulus, CVR_{DELAY}. Measures between time points in patients with good and poor surgical outcomes based on DSA-visualized neoangiogenesis were contrasted (signed-rank test; significance: 2-sided $P < .050$).

RESULTS: $rCVR_{RAW}$ increases ($P = .010$) and CVR_{DELAY} decreases ($P = .001$) were observed pre- vs post-revascularization in hemispheres with DSA-confirmed collateral formation; no difference was found pre- vs post-revascularization in hemispheres with poor revascularization. No significant change in $rCVR_{MAX}$ post-revascularization was observed in either group, or between any of the MRI measures, in the nonsurgical hemisphere.

CONCLUSION: Improvement in parenchymal compliance measures post-revascularization, primarily attributed to reductions in microvascular response time, is concurrent with collateral formation visualized on DSA, and may be useful for longitudinal monitoring of surgical outcomes.

KEYWORDS: Cerebral blood flow, Cerebrovascular reactivity, Intracranial stenosis, Moyamoya disease, Stroke

Neurosurgery 84:261–271, 2019 DOI:10.1093/neuros/nyx635 www.neurosurgery-online.com

Moyamoya is characterized by progressive stenosis of the supraclinoid internal carotid arteries (ICAs) and their proximal branches, and the development of compensatory collaterals.[1] There is currently no medical treatment that is known to halt or reverse moyamoya, and treatment focuses on improving cerebral blood flow

ABBREVIATIONS: ACT, arterial circulation time; **ASL,** arterial spin labeling; **BOLD,** blood oxygenation level-dependent; **CBF,** cerebral blood flow; **CBV,** cerebral blood volume; **CVR,** cerebrovascular reactivity; **DSA,** digital subtraction angiography; **EDAS,** encephaloduroarteriosynangiosis; **EMS,** encephalomyosynangiosis; **$EtCO_2$,** end-tidal CO_2; **FLAIR,** fluid-attenuated inversion recovery; **FSL,** FMRIB Software Library; **ICA,** internal carotid artery; **MCA,** middle cerebral artery; **MRI,** magnetic resonance imaging; **mSS,** modified Suzuki Score; **rCVR,** relative CVR; **STA,** superficial temporal artery; **TE,** echo time; **TI,** inversion time; **TR,** repetition time

Supplemental digital content is available for this article at www.neurosurgery-online.com.

(CBF, mL blood/100g tissue/min) through surgical revascularization.[2,3] There is increasing evidence that revascularization improves outcomes in patients with moyamoya[4-6]; however, due to limited imaging approaches that can objectively assess outcomes with minimal risk, the temporal course of cerebral hemodynamic improvement following surgery is generally not well characterized, and rather, success is determined more coarsely based on changes in symptomatology, recurrent stroke, or a single or limited number of surveillance angiograms. Additionally, a limited number of studies have been performed directly comparing outcomes of direct vs indirect surgical approaches,[7-9] and it is logical that personal vascular and tissue profiles could be used to triage patients for the most beneficial approach.

One limitation to performing formal efficacy trials is that surgical success is most commonly evaluated qualitatively through changes in symptomatology or collateral visualization on digital subtraction angiography (DSA). While DSA is useful for anatomical visualization of the collateral network, it provides limited spatial information and is insensitive to tissue-level changes in CBF. Additionally, DSA requires ionizing radiation and carries procedural risks, and thus may not be performed for long-term surveillance. As a result, the mechanism and temporal course of how revascularization surgery impacts parenchyma function is not well characterized; alternative imaging approaches that can provide comparable or additional information to DSA would be helpful.

One promising approach is hypercapnic cerebrovascular reactivity (CVR)-weighted mapping.[10-14] The premise underlying CVR-weighted mapping is that reductions in cerebral perfusion pressure secondary to arterial steno-occlusion may be compensated for at the tissue level by autoregulatory increases in cerebral blood volume (CBV, mL blood/100g tissue). By challenging vessels with a vasodilatory stimulus (eg, acetazolamide, breath hold, or mild hypercapnia), it is possible to evaluate the corresponding hyperemic response, which will be attenuated in parenchyma operating at or near autoregulatory reserve capacity. This approach has been applied in single-photon emission computed tomography[15-17] and MRI-CBF[18-22] studies; however, these methods require exogenous contrast, ionizing radiation, or possess low sensitivity to delayed blood-arrival time.

Noninvasive hypercapnic blood oxygenation level-dependent (BOLD)-MRI, which provides a qualitative surrogate of CBF and CBV changes, can be applied to record changes in tissue-level hemodynamics over a longer blood-arrival and vascular response time. It has recently been suggested that neoangiogenic collateral arterioles formed due to cerebrovascular disease may have distinct vasoactive properties relative to healthy arterioles.[23] This suggests that not only the magnitude of the change in parenchymal blood volume and flow, commonly referred to as CVR, but also the time for parenchymal vessels to respond maximally to vasoactive stimuli or progressive reductions in cerebral perfusion pressure, may represent distinct features of parenchymal health. Both constructs can be evaluated noninvasively[24] and may provide information on revascularization success.

Importantly, there is a clinical need for noninvasive methods to monitor surgical outcomes in patients with moyamoya, but first these methods must be compared directly with accepted angiographic techniques. Here, we evaluated moyamoya patients using gold-standard DSA and hypercapnic BOLD-MRI before and after surgical revascularization. Our first objective was to understand the relationship between collateral formation from DSA and the change in MRI-measured CVR using a conventional analysis. A secondary objective was to apply a novel time-delay analysis to the MRI data to understand whether (i) the magnitude of the vascular response or (ii) the time delay to maximal vascular response provided the best revascularization response indicator. The goal was to determine whether these MRI parameters provide similar information to DSA collateralization extent and thus provide noninvasive surrogates of revascularization success.

METHODS

The study was approved by the institutional review board. Patients presenting to the clinical neurosurgery services between March 2011 and March 2016 with suspected moyamoya underwent a protocol of DSA and BOLD-MRI, and any patient with symptomatic moyamoya underwent revascularization as part of clinical standard of care. Decision regarding direct vs indirect revascularization was made based on the caliber of the superficial temporal artery (STA). Revascularized patients underwent postoperative DSA and follow-up BOLD-MRI at approximately 12 mo post-surgery 68 patients with a diagnosis of moyamoya from DSA were identified during this time period of which 66 patients provided consent to participate in research. The 66 patients were then evaluated for the following inclusion criteria for this cohort analysis: (i) revascularization of 1 or both hemispheres; (ii) pre- and post-surgical DSA; (iii) pre- and post-surgical BOLD-MRI. Healthy adults (n = 9) age matched within 1 decade of life to moyamoya participants also provided consent and were enrolled for reference evaluation of the BOLD-MRI measurement.

Surgical Revascularization

All surgical revascularizations were indirect, with the exception of one where the patient presented with multiple crescendo-type ischemic symptoms and the STA caliber was large, and therefore a direct STA to middle cerebral artery (MCA) bypass was performed. The indirect procedures were encephaloduroarteriosynangiosis (EDAS) type, in which the STA was sutured either directly to the cortex or dura, and one procedure was encephalomyosynangiosis (EMS), which was similar to EDAS; however, instead of dissection of the STA, the temporalis muscle with associated vasculature was dissected and placed onto the surface of the brain. EMS was performed in this patient due to low STA caliber, but sufficient temporalis graft muscle. As the purpose of this study was to evaluate consistency between DSA and MRI, rather than how the type of surgical revascularization impacted collateral formation, subtype of surgical revascularization was not an exclusion criterion.

Image Acquisition

MRI was performed on a 3.0T Achieva scanner (Philips Healthcare, Best, The Netherlands).

Digital Subtraction Angiography

Moyamoya participants underwent diagnostic DSA with catheterization and injection with intra-arterial contrast of bilateral common carotid arteries, external carotid arteries when feasible, ICAs when feasible, and vertebral arteries.

Anatomical Imaging

T_2-weighted fluid-attenuated inversion recovery (FLAIR; spatial resolution = 0.91 × 0.99 × 5.0 mm^3; repetition time (TR)/echo time (TE)/inversion time (TI) = 11000/120/2800 ms), 3-dimensional T_1-weighted (spatial resolution = 1.0 × 1.0 × 1.0 mm^3; TR/TE = 9.0/4.6 ms), and diffusion-weighted (spatial resolution = 0.9 × 0.9 × 5.0 mm^3; TR/TE 9636.6/92.6 ms, b = 0 and b = 1000 s/mm^2) imaging were performed for infarct determination.

Cerebrovascular Reactivity-Weighted Imaging

CVR-weighted images were obtained as previously described using a paradigm consisting of 2 3-min blocks of carbogen (5% CO_2, 95% O_2), interleaved with room air.[25,26] In control subjects, we evaluated both carbogen and hypercarbic normoxia using identical block paradigms to understand effect on output metrics. Whole-brain (slices = 31) single-shot gradient echo echo-planar-imaging BOLD images were acquired with spatial resolution = 3.0 × 3.0 × 3.5 mm^3 and TR/TE = 2000/35 ms.

Analysis

Digital Subtraction Angiography

Hemispheric modified Suzuki Score (mSS) was determined by a board-certified neuroradiologist (LTD) and neurosurgeon (MRF). For mSS grading, the range was 0 to 4, with 0 representing no steno-occlusive changes and 4 representing complete occlusion of both proximal anterior and MCAs.[1,27] Revascularization success was determined by DSA based on the amount of the MCA territory revascularized as described in Figure 1. One board-certified neuroradiologist and 1 board-certified neurosurgeon, blinded to results of cerebrovascular imaging, performed the scoring from DSA together and provided a consensus score, which was preserved for comparison with MRI data.

Anatomical Imaging

A board-certified neuroradiologist evaluated images for presence and size of chronic infarcts (FLAIR hyperintense lesions ≥ 3 mm with T_1 hypointensity approaching cerebrospinal fluid signal). Acute infarcts were assessed by the same neuroradiologist using diffusion-weighted imaging and standard clinical criteria.[28]

Cerebrovascular Reactivity-Weighted Imaging

Data were preprocessed using FSL software[29] to correct for motion (affine; degrees of freedom = 6) and baseline drift (high-pass filtering at 0.0028 Hz). The vascular compliance measures were generated using 2 different approaches. First, conventional CVR maps were generated based on the calculated z-statistic between the voxel time course and a standard static rectangular regressor that corresponded in time with the gas stimulus paradigm. Voxelwise z-statistics were then normalized by dividing by the mean z-statistic in the bilateral posterior circulation flow territory to allow for group-level analysis of changes in relative CVR ($rCVR_{RAW}$). The premise underlying this normalization procedure is that posterior involvement is less common in moyamoya and therefore this region provides a less-involved control region. However, in one patient a unilateral posterior cerebral artery stenosis was present, and in this patient only the contralateral posterior flow territory without significant stenosis was used for normalization.

The assumption, which is not necessarily true and is investigated here, is that all voxels increase at a similar time, and the only relevant contributors to the z-statistic are the magnitude response and time-course noise. We also performed time-delay analysis[24] to understand the separate contribution from parenchymal response times and the magnitude of the response. Here, the above regressor corresponding to the gas stimulus paradigm was progressed in time and we recorded the time at which maximum correlation occurs between each voxelwise BOLD time course and the regressor (CVR_{DELAY}), as well as the corresponding maximum z-statistic (CVR_{MAX}). This maximum z-statistic was then normalized by the mean of the maximum z-statistics over the posterior circulation territories, as described above, to generate a $rCVR_{MAX}$ value. This time-delay analysis allowed for decomposition of the CVR-weighted response into the time required for the vessels to respond maximally to the stimulus as well as a statistical measure of this maximum response, which correlates with the maximum signal change. Note that vascular compliance

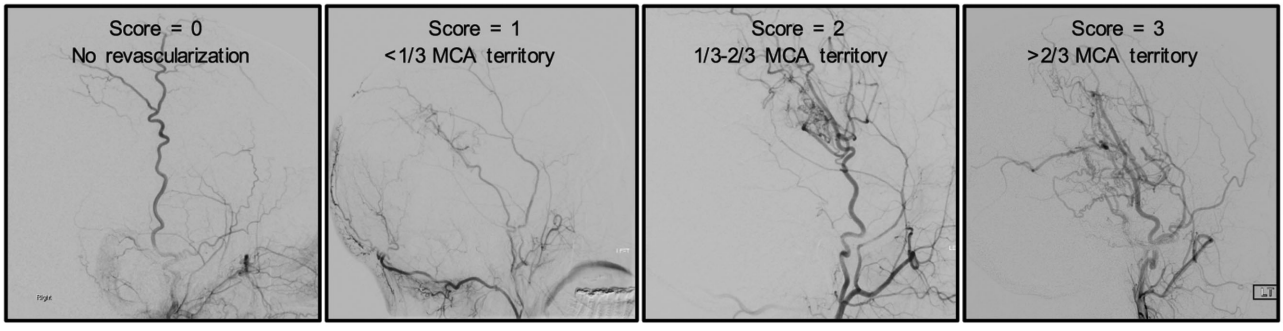

FIGURE 1. *Scoring system for evaluation of revascularization. Lateral projections from DSA were used to assess revascularization success of the middle cerebral artery (MCA) territory. The 4 categories used for classification were based on previously established Matsushima scoring system: 0: no revascularization, 1: <1/3 of the MCA territory, 2: 1/3 to 2/3 of MCA territory, and 3: >2/3 of the MCA territory.*

times may not be temporally correlated with end-tidal CO_2 ($EtCO_2$) changes due to differences in blood-arrival time, and/or smooth muscle and endothelial dysfunction, and this secondary analysis provides a distinct data-driven construct that does not rely on the assumption that vascular compliance changes and $EtCO_2$ dynamics are temporally correlated identically for all brain voxels. Representative BOLD time courses and combined $rCVR_{RAW}$, $rCVR_{MAX}$ and CVR_{DELAY} maps are shown in Figure 2.

Image Registration and Regions of Interest

Data were co-registered to a 2-mm Montreal Neurological Institute T_1-weighted standard space atlas,[30] and mean values were calculated in the MCA territory of the operative hemisphere pre- and post-revascularization (**Figure**, **Supplemental Digital Content 1**).[31] Nonoperative hemispheres and control subjects were also evaluated in an identical fashion. CVR metrics in MCA territories were preserved for hypothesis testing.

Statistical Concerns

The primary hypothesis was that participants with successful revascularization, defined as neovascularization on DSA that covers >1/3 of the MCA territory, will have increased postoperative, relative to preoperative, $rCVR_{RAW}$ values. A secondary aim was to evaluate the effect of surgical revascularization on novel vascular compliance metrics, $rCVR_{MAX}$ and CVR_{DELAY}. To test both study objectives, patients were divided into those with >1/3 MCA territory revascularized vs those with <1/3 MCA territory revascularized and a 2-sided Wilcoxon signed-rank test was used to compare hemispheric $rCVR_{RAW}$, $rCVR_{MAX}$, and CVR_{DELAY} between pre-surgical and post-surgical time points. Two-tailed P-value < .050 was required for significance.

RESULTS

Demographics

Table 1 summarizes demographic information of the moyamoya cohort. Twenty-six brain hemispheres from 17 patients met inclusion criteria. Three patients were excluded due to technical issues: 1 patient due to suboptimal $EtCO_2$ changes (<3 mm Hg increase in response to carbogen) from the gas delivery (likely due to poor mask fitting), 1 patient due to an implanted screw that caused a large artifact, and 1 patient due to claustrophobia and inability to complete the scan. Therefore, 20 total operative hemispheres from 14 participants were included.

BOLD-MRI data were evaluated at 13.9 ± 6.6 mo post-revascularization, and collateralization on DSA was evaluated at 12.8 ± 4.8 mo post-revascularization. The time between follow-up DSA and follow-up BOLD-MRI was 2.8 ± 4.5 mo. There was no significant difference in $EtCO_2$ change when comparing pre-surgical with post-surgical scans ($P = .270$). A significant correlation between all vascular compliance measures using hypercapnic normoxia and hypercapnic hyperoxia (eg, carbogen) in control subjects was observed (**Figure**, **Supplemental Digital Content 2**).

Revascularization Response

Revascularization success in the included hemispheres using the DSA grading system of 0/1/2/3 yielded categorization of 1/4/12/3 hemispheres, respectively.

Vascular Compliance Measures in Healthy Participants and Patients With Moyamoya

Group-level composite maps of vascular compliance measures in control participants and pre-surgical moyamoya participants are shown in Figure 3. Bilaterally decreased $rCVR_{RAW}$ and $rCVR_{MAX}$, and increased CVR_{DELAY}, values in moyamoya vs control participants were observed.

Vascular Compliance Measures Pre- and Post-revascularization

Group-level vascular compliance measures in operative hemispheres are shown in Table 2. Consistent with the primary hypothesis, $rCVR_{RAW}$ increased following surgical revascularization in the cohort with >1/3 MCA territory neovascularization (pre-surgery $rCVR_{RAW} = 0.46 \pm 0.26$; post-surgery $rCVR_{RAW} = 0.63 \pm 0.12$; $P = .010$). In participants with <1/3 MCA territory revascularized, there was no significant change in $rCVR_{RAW}$ (pre-revascularization $rCVR_{RAW} = 0.59 \pm 0.20$; post-revascularization $rCVR_{RAW} = 0.58 \pm 0.24$; $P > .500$). There was no significant change in $rCVR_{MAX}$ in either group.

In participants with >1/3 MCA territory revascularized, a significant decrease in CVR_{DELAY} was found following revascularization (pre-revascularization $CVR_{DELAY} = 57.9 \pm 13.6$ s; post-revascularization $CVR_{DELAY} = 49.0 \pm 8.2$ s; $P = .001$). In participants with <1/3 MCA territory revascularized, no significant change in CVR_{DELAY} was found (pre-revascularization $CVR_{DELAY} = 50.4 \pm 6.0$s; post-revascularization $CVR_{DELAY} = 52.9 \pm 14.3$ s; $P > .500$). Therefore, when considering the operative hemisphere in participants who had >1/3 MCA territory revascularized, both $rCVR_{RAW}$ and CVR_{DELAY} were discriminatory on average for determining surgical outcome. No significant difference in any vascular compliance measure was observed in the nonrevascularized hemispheres. Figure 4 shows case examples (for additional slices, see **Figure**, **Supplemental Digital Content 3**). Pre- and post-surgical vascular compliance measures are shown in Figure 5.

Group-level maps of vascular compliance measures are shown in Figure 6. $rCVR_{RAW}$ values increase and CVR_{DELAY} values decrease only in hemispheres with >1/3 MCA territory revascularization, whereas $rCVR_{MAX}$ values were not observed to change significantly.

DISCUSSION

While studies of CVR changes in response to surgical revascularization in moyamoya have been performed,[32-34] CVR has never been compared longitudinally with collateral changes on gold-standard DSA. We applied traditional CVR and novel

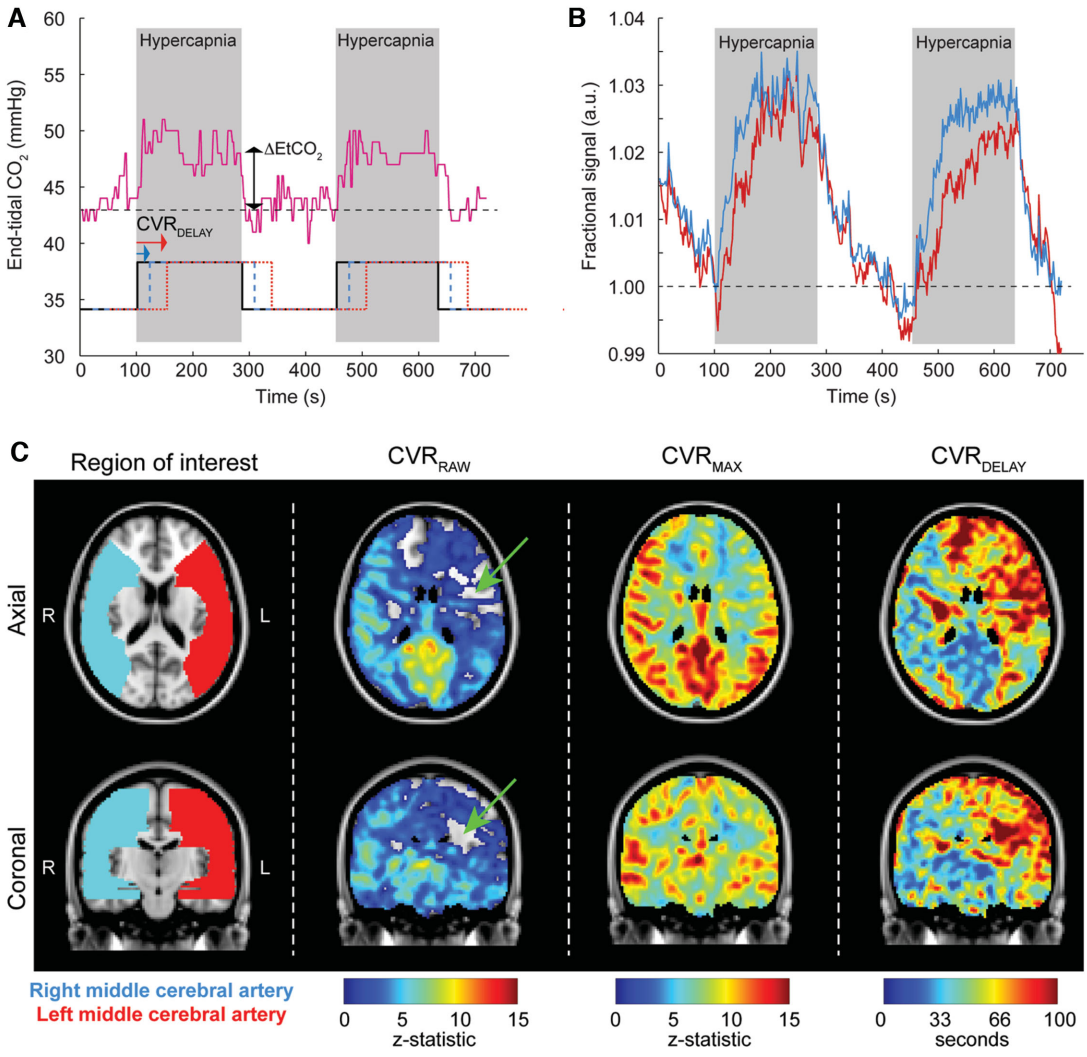

FIGURE 2. *Multiparametric quantification of the hypercapnic blood oxygenation level-dependent (BOLD) response. This analysis allows for decomposition of the cerebrovascular reactivity (CVR)-weighted response into the time required for the vessels to respond maximally to the stimulus as well as a statistical measure of this maximum response, which correlates with the maximum signal change. The stimulus paradigm utilizes 2 180s blocks of hypercapnia (5% CO_2/95% O_2) interleaved with 180 s of baseline medical air (~21% O_2/~79% N_2).* **A**, *This hypercapnic stimulus elicits an approximately 5 to 7 mm Hg increase in end-tidal CO_2 ($EtCO_2$), shown here for a 54-yr-old female moyamoya patient with right-sided neurological symptoms. Conventional CVR (CVR_{RAW}) describes the z-statistic between the voxel-wise time course and a regressor that corresponds in time with the administered gas paradigm (black solid). Stronger correlation between the regressor and the BOLD time course results in higher CVR_{RAW} values. It is also possible to progress the regressor in time (blue and red) and calculate the corresponding z-statistic for each time progression element. In this time-delay analysis, the maximum z-statistic (CVR_{MAX}) and corresponding time in seconds the regressor has been progressed (CVR_{DELAY}) can be recorded in a manner that accounts for different times for the reactivity response. In a patient with moyamoya, both the magnitude and delay times may differ in a manner that depends on autoregulatory reserve capacity and vascular compliance timing.* **B**, *The blue time course is from the right MCA territory and the red time course is from the left MCA territory in the same patient with right-sided neurological symptoms. The CVR_{MAX} is reduced and CVR_{DELAY} lengthened throughout the left MCA territory.* **C**, *Axial and coronal representations of the CVR_{RAW} (z-statistic from the regressor that corresponds in time with the stimulus; black), as well as the decomposed CVR_{MAX} and CVR_{DELAY}. It can be seen that apparent negative CVR_{RAW} in some voxels (green arrows) can be explained by substantially elongated CVR_{DELAY} values. This time regression analysis provides a more complete perspective on the hemodynamic reactivity and timing values than is obtained from conventional analyses, which utilize only the $EtCO_2$ time course or stimulus paradigm as the regressor.*

TABLE 1. Demographics of Moyamoya Patients

Parameter	Moyamoya (n = 14)
Age (years, mean ± std. dev.) (range)	38 ± 14 (16-59)
Biological sex (% female)	93 (13/14)
Race (% Asian/white/black)	7.1/71.4/21.4
Antiplatelet (% on therapy)	57.1
Cardiovascular risk factors	57.1
Diabetes mellitus (%)	14.3
Smoking (%)	21.4
Modified Suzuki Score right (mean ± std. dev.)	2.3 ± 1.0
Modified Suzuki Score left (mean ± std. dev.)	2.1 ± 1.0
Idiopathic Moyamoya (%)	78.6
Change in end-tidal CO_2 (mmHg, mean ± std. dev.)	6.0 ± 1.6
Infarct at presentation (%)	78.6
New infarct at follow-up (%)	14.3

time-delay BOLD image processing in patients with moyamoya before and after surgical revascularization and found that changes in parenchymal vascular compliance measures, specifically $rCVR_{RAW}$ and CVR_{DELAY}, were consistent with collateral formation on DSA.

Time-delay processing of BOLD may provide additional information beyond more qualitative measures such as signal change. Our findings are consistent with prior reports that found a traditional CVR analysis to be sensitive to surgical response to revascularization,[32] but we extend this analysis to include more specific temporal features of the BOLD hemodynamic response function. In participants with >1/3 MCA territory revascularized, the significant decrease in CVR_{DELAY} coupled with no significant change in $rCVR_{MAX}$ at the group level may indicate that the absolute reserve capacity (ability to accommodate increases in CBF in response to hypercapnia) in territories fed by vessels with arterial vasculopathy is often not exhausted, but rather that reactivity time delay may be prolonged and may play a large role in apparent decreased reactivity values as evaluated by traditional analysis. Therefore, while static regression analysis is simple, and the most common BOLD CVR analysis variant, such results in the setting of vascular disease should be interpreted with caution, as apparent CVR decreases may be partly or wholly due to delayed smooth muscle compliance. Furthermore, when stimuli of short duration are used, or $EtCO_2$ time courses are used for regression analysis, it is possible that CVR is underestimated if vascular reactivity delays are lengthened. In extreme cases, these conventional analyses could even lead to duplicitous negative signal changes (eg, Figure 2), often attributed to vascular steal phenomena, owing to the poststimulus signal being larger than the stimulus signal and lengthened CVR_{DELAY}. Most CVR-MRI approaches apply either arterial spin labeling (ASL)-MRI, which has lower temporal resolution (4-8 s) and has low sensitivity to delayed blood-arrival times beyond the T_1 of arterial blood water (eg, 1.6-1.8 s at 3T) at typical postlabeling delays of 1.5 to 2.0 s, or BOLD-MRI that is performed for much shorter stimulus durations and uses only the gas paradigm or $EtCO_2$ time course as a regressor. Of note, CVR_{DELAY} is a measure that is absolute, and reported in seconds (relative to stimulus start, which is the same between subjects), and other similar measures of reactivity delay such as $CVR_{lagtime}$ have been described. $CVR_{lagtime}$ is measured relative to the participant's global hemodynamic response. In scenarios of widespread vascular impairment, such as moyamoya, the global response function may itself be abnormal, making this approach more complex to interpret. In this study, we additionally evaluated consistency between CVR_{DELAY} and $CVR_{lagtime}$ and found that these measures were significantly correlated on average across subjects ($P < .050$).

Here, we provide evaluation of the functional underpinnings of newly formed vessels by performing traditional and time-delay CVR analysis. It is possible that the newly formed smooth muscle lined arterioles are capable of a more rapid response to changes in $PaCO_2$ and pH which results in increased traditional CVR measurements and decreased reactivity delay. Of note, reactivity

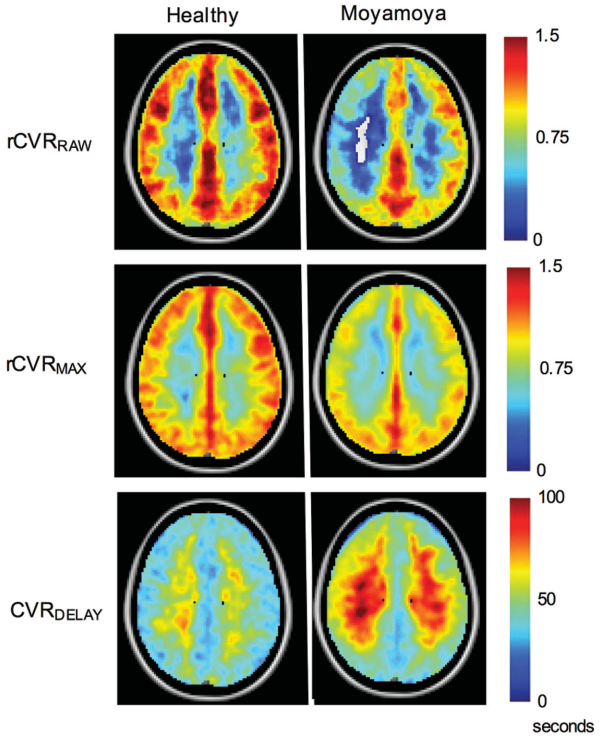

FIGURE 3. *Group-level maps of vascular compliance measures in healthy control participants and pre-surgical moyamoya participants. Single axial views of each group-averaged vascular compliance measure are shown. Bilaterally decreased $rCVR_{RAW}$ and $rCVR_{MAX}$ and bilaterally increased CVR_{DELAY} values can be seen. Consistent with moyamoya pathology, $rCVR_{RAW}$ and $rCVR_{MAX}$ are increased posteriorly compared to in middle and anterior cerebral artery territories. Vessel reactivity time as reflected in the CVR_{DELAY} maps is longer in the deep white matter compared to cortical gray matter in both the control and moyamoya participant groups.*

TABLE 2. Pre- and Post-surgical Cerebrovascular Compliance Measures Separated by Hemispheres With >1/3 MCA Territory Revascularization and <1/3 MCA Territory Revascularization

	>1/3 MCA territory revascularization (n = 14 hemispheres)		<1/3 MCA territory revascularization (n = 5 hemispheres)	
Vascular compliance measures	**Pre-surgery**	**Post-surgery**	**Pre-surgery**	**Post-surgery**
$rCVR_{RAW}$; mean ± std. dev. (range)	0.46 ± 0.26 (−0.19 to 0.79)	0.63 ± 0.12 (0.40 to 0.83)	0.59 ± 0.20 (0.38 to 0.88)	0.58 ± 0.24 (0.31 to 0.85)
$rCVR_{MAX}$; mean ± std. dev. (range)	0.83 ± 0.07 (0.71 to 0.95)	0.86 ± 0.06 (0.75 to 0.95)	0.88 ± 0.12 (0.67 to 0.96)	0.86 ± 0.12 (0.72 to 0.98)
CVR_{DELAY}; mean ± std. dev. (range)	57.94 ± 13.61 (34.73 to 83.71) s	49.10 ± 8.19 (33.65 to 66.59) s	50.40 ± 5.98 (45.63 to 60.70) s	52.90 ± 14.31 (37.74 to 72.46) s

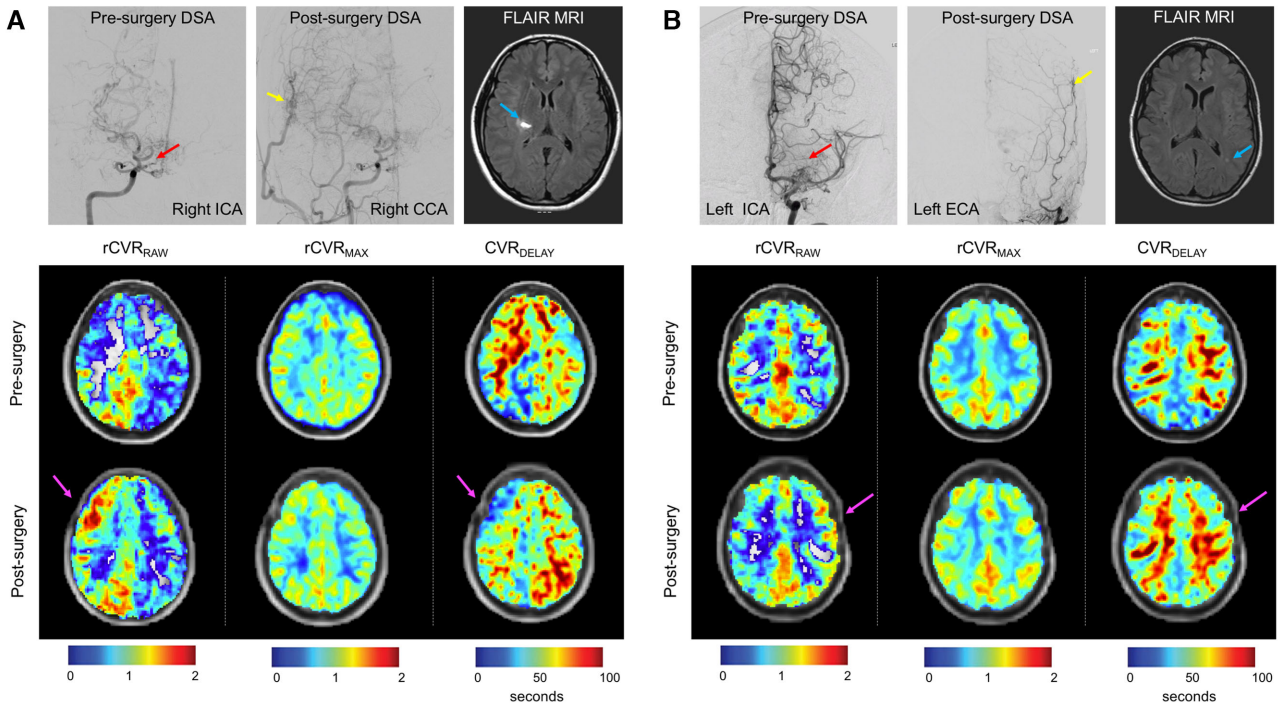

FIGURE 4. *Individual cases of DSA and vascular compliance imaging pre-and post-surgical revascularization.* **A**, *A participant with robust post-surgical revascularization of the right MCA territory; shown are anterior-posterior projections of the internal carotid artery (ICA), common carotid artery (CCA), and external carotid artery (ECA) injections. The red arrow denotes moyamoya collaterals in the pre-surgical image, and the yellow arrow shows the region of neovascularization. This patient presented with an infarct in the right hemisphere (blue arrow). Additional panels below show correspondent BOLD-derived vascular compliance measures. Increases in $rCVR_{RAW}$, and more modest increases in $rCVR_{MAX}$ can be seen, and decreases in CVR_{DELAY} are observed post-surgery in the right hemisphere (magenta arrows denote surgical location).* **B**, *In contrast, a participant with minimal post-surgical neovascularization following left-sided surgery is shown. This patient presented with a left-sided infarct which appears as a punctate FLAIR hyperintense lesion in the white matter (blue arrow). Corresponding BOLD-MRI-derived vascular compliance measures show decreases in left-sided $rCVR_{RAW}$, stable $rCVR_{MAX}$, and increases in CVR_{DELAY}.*

delay values greatly exceed arterial circulation time (ACT) even in patients with steno-occlusion and delayed filling due to collateral pathways (wherein ACT ~3 s).[22] Using time-delay regression, we report a metric indicative of the ACT and maximal microvascular dilation time (>20 s in some vessels). Additionally, in support of the hypothesis that neovascularization contributes to decreased time delay and increased reactivity, a recent cadaveric evaluation of the arteriogenesis 22 years after indirect revascularization

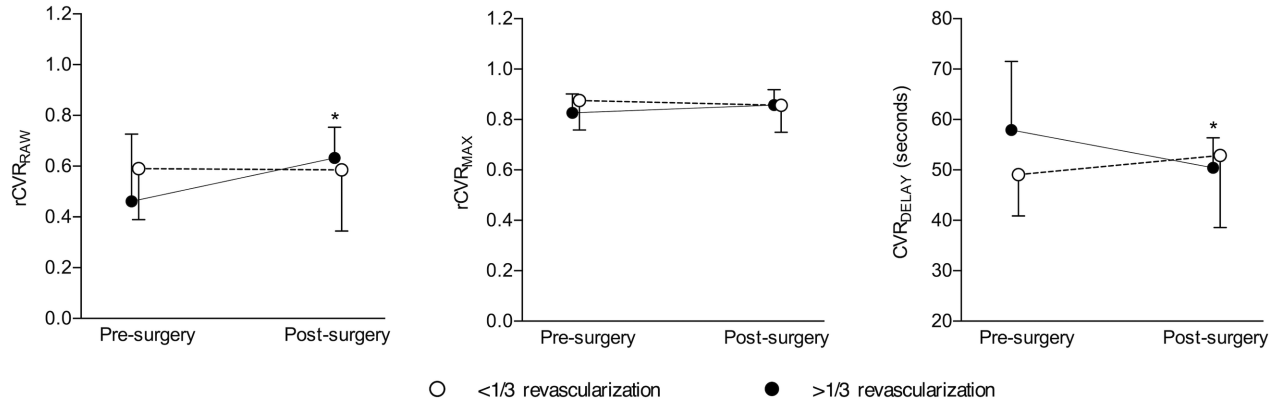

FIGURE 5. *Group-level results of vascular compliance measures. A 2-sided Wilcoxon signed-rank test was performed to test the primary hypothesis that improvements in MCA territory $rCVR_{RAW}$ will be present in hemispheres with >1/3 MCA territory revascularization. The secondary aim was to evaluate changes in $rCVR_{MAX}$ and CVR_{DELAY} in patients following surgery. An increase in $rCVR_{RAW}$ in participants with >1/3 MCA territory revascularization ($P = .010$) and no significant change in $rCVR_{RAW}$ in participants with <1/3 MCA territory revascularization was observed. No significant change was observed in $rCVR_{MAX}$ in participants classified in either group. A decrease in CVR_{DELAY} in hemispheres with >1/3 MCA territory revascularization ($P = .001$) and no significant change in CVR_{DELAY} in participants with <1/3 MCA territory revascularization was observed. For clarity, the group-level mean +1 or −1 standard deviation is shown for each vascular compliance measure pre- and post-surgery.*

showed that the formed vessels had the characteristic 3-layer arterial wall anatomy (with smooth muscle actin contributing to the medial layer).[35]

There is a clinical need for noninvasive tools to monitor surgical outcomes in moyamoya patients, as many patients with this condition are diagnosed at young ages, and serial imaging using ionizing radiation involves risks over the lifespan. CVR studies using low levels of carbon dioxide are safe, well tolerated, feasible on clinical scanners without using exogenous contrast or special instrumentation,[12,25] and minimally affected by most craniotomy hardware.[36] Also, this method allows for larger spatial coverage, and reflects tissue-level function of collateral vessels vs large vessel patency alone. The respiratory stimulus that was exploited in this study allows for rapid, repeatable $PaCO_2$ modulations, thereby allowing sensitive interrogation of temporal parameters (eg, CVR_{DELAY}) of the hemodynamic response function. Alternative clinical methods for evaluating CVR often exploit intravenous acetazolamide administration. Both hypercapnia and acetazolamide are anticipated to yield pH-induced changes in vasodilation, and through similar mechanistic pathways decrease perivascular pH as a result of increasing blood $PaCO_2$. Hypercapnia offers additional advantages including its noninvasive nature, the ability to turn it on and off quickly in a single scan session to evaluate vascular timing parameters, and reduced concerns related to dose restrictions or drug interactions.

Limitations

There are several limitations that should be considered. First, our sample size for participants with minimal revascularization is limited, and we may be underpowered to robustly evaluate post-surgical changes in this group. Second, more quantitative approaches such as ASL have been evaluated in revascularized patients, and have the advantage of yielding measures of CBF in mL/100 g tissue/min.[18,37] However, ASL is of limited use with recommended parameters when blood-arrival times are delayed more than a few seconds, due to the lifetime of the magnetic blood water label ($T_{1,blood}$ = 1.6-1.8 s at 3T [38]). In the composite maps of the vascular compliance measures, many of the regional changes were observed in the deep white matter, which due to delayed blood-arrival time cannot be accurately measured by ASL approaches at 3T.[39] Third, evaluating changes in neurological symptoms in this patient cohort is complex. This is because persistent symptoms may be present as a result of old infarcts despite surgical success, and we found that ongoing symptoms (eg, headache, fatigue, etc.) are often diffuse, with changes in severity difficult to assess objectively. We did evaluate the presence of new strokes at follow-up, and found that 14.3% of the patients had a new infarct. A future study could focus on longer-term monitoring to evaluate the presence of new or recurrent overt or silent infarcts. Fourth, pre-surgical $rCVR_{RAW}$, as analyzed by traditional static regressor analysis, differed between the group with >1/3 (0.46 ± 0.26) and <1/3 revascularization of the MCA territory ($rCVR_{RAW} = 0.59 \pm 0.20$). Although this difference did not meet criteria for significance ($P = .330$), other studies have shown that preoperative CVR is predictive of surgical outcome with patients with lower preoperative CVR having greater benefit from surgery on follow-up vascular compliance imaging.[33] Fifth, we focused on statistical measures, rather than absolute signal changes, as these have been shown to be better indicators of lateralizing disease in these patients using this stimulus, although CVR and signal change measures are significantly correlated as expected (**Figure**, **Supplemental Digital Content 4**).[25] Finally, at

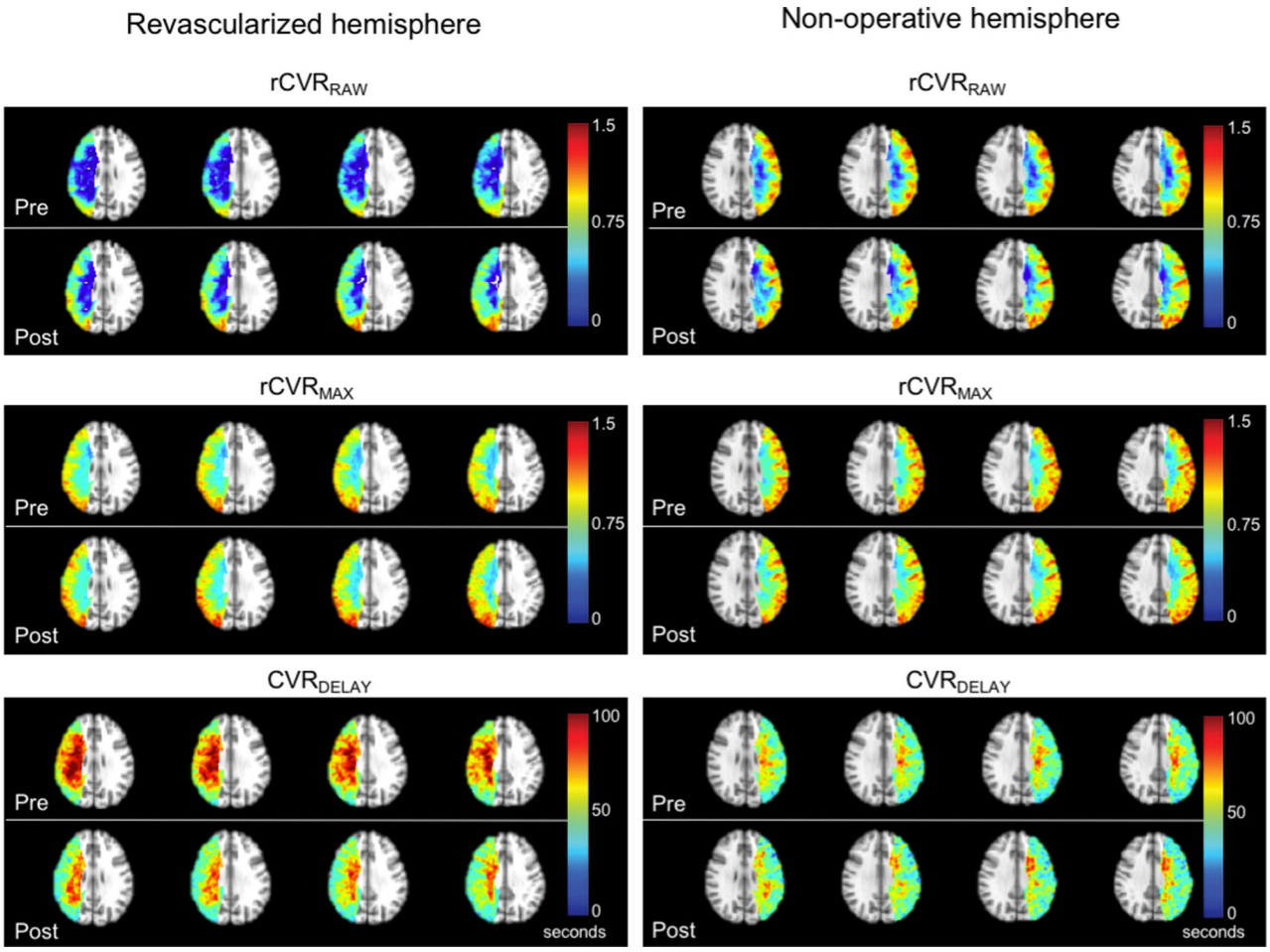

FIGURE 6. *Group-level maps of vascular compliance measures in operative and non-operative hemispheres. Maps of revascularized hemispheres (>1/3 MCA territory) and maps of non-operative hemispheres are shown. Increased rCVR$_{RAW}$, marginally increased rCVR$_{MAX}$, and decreased CVR$_{DELAY}$ are observed following revascularization. In non-operative hemispheres, no significant changes in rCVR$_{RAW}$, rCVR$_{MAX}$, or CVR$_{DELAY}$ were observed on average.*

our center, noninvasive hypercapnic BOLD imaging is performed on pre- and post-surgical moyamoya patients. While 1-yr post-surgical DSA is still performed to evaluate collateral formation, we anticipate noninvasive BOLD imaging to be a complement and potential alternative to DSA post-surgically. A larger cohort of patients would be required to evaluate cut-off values and determine the sensitivity and specificity of changes in vascular compliance measures for determining revascularization success; encouraging preliminary receiver operating characteristic curve analysis is provided in **Figure**, **Supplemental Digital Content 5**.

CONCLUSION

We applied traditional CVR and novel time-delay BOLD image processing in patients with moyamoya before and after surgical revascularization in addition to DSA evaluation of collateral vessels. Neovascularization as seen on DSA was associated with parenchymal improvements in vascular compliance measures as determined by traditional regressor and reactivity time-delay approaches. Traditional and time-delay analysis of CVR data may provide a noninvasive tool for monitoring revascularization success.

Disclosures

Funding was from NIH/NINDS (5R01NS078828 and 5R01NS097763) and NIH/NIGMS (T32GM007347). The authors have no personal, financial, or institutional interest in any of the drugs, materials, or devices described in this article.

REFERENCES

1. Scott RM, Smith ER. Moyamoya disease and moyamoya syndrome. *N Engl J Med*. 2009;360(12):1226-1237.

2. Agarwalla PK, Stapleton CJ, Phillips MT, Walcott BP, Venteicher AS, Ogilvy CS. Surgical outcomes following encephaloduroarteriosynangiosis in north american adults with moyamoya. *J Neurosurg*. 2014;121(6):1394-1400.
3. Mallory GW, Bower RS, Nwojo ME, et al. Surgical outcomes and predictors of stroke in a north american white and african american moyamoya population. *Neurosurgery*. 2013;73(6):984-992; discussion 981-982.
4. Kim T, Oh CW, Kwon OK, et al. Stroke prevention by direct revascularization for patients with adult-onset moyamoya disease presenting with ischemia. *J Neurosurg*. 2016;124(6):1788-1793.
5. Guzman R, Lee M, Achrol A, et al. Clinical outcome after 450 revascularization procedures for moyamoya disease. Clinical article. *J Neurosurg*. 2009;111(5):927-935.
6. Bao XY, Duan L, Yang WZ, et al. Clinical features, surgical treatment, and long-term outcome in pediatric patients with moyamoya disease in china. *Cerebrovasc Dis*. 2015;39(2):75-81.
7. Kazumata K, Ito M, Tokairin K, et al. The frequency of postoperative stroke in moyamoya disease following combined revascularization: A single-university series and systematic review. *J Neurosurg*. 2014;121(2):432-440.
8. Sadashiva N, Reddy YV, Arima A, Saini J, Shukla D, Pandey P. Moyamoya disease: experience with direct and indirect revascularization in 70 patients from a nonendemic region. *Neurol India*. 2016;64(suppl):S78-S86.
9. Wang L, Qian C, Yu X, et al. Indirect bypass surgery may be more beneficial for symptomatic patients with moyamoya disease at early suzuki stage. *World Neurosurg*. 2016;95:304-308.
10. Ziyeh S, Rick J, Reinhard M, Hetzel A, Mader I, Speck O. Blood oxygen level-dependent mri of cerebral co2 reactivity in severe carotid stenosis and occlusion. *Stroke*. 2005;36(4):751-756.
11. Griffeth VE, Buxton RB. A theoretical framework for estimating cerebral oxygen metabolism changes using the calibrated-bold method: Modeling the effects of blood volume distribution, hematocrit, oxygen extraction fraction, and tissue signal properties on the bold signal. *NeuroImage*. 2011;58(1):198-212.
12. Spano VR, Mandell DM, Poublanc J, et al. CO_2 blood oxygen level-dependent mr mapping of cerebrovascular reserve in a clinical population: safety, tolerability, and technical feasibility. *Radiology*. 2013;266(2):592-598.
13. Fisher JA, Sobczyk O, Crawley A, et al. Assessing cerebrovascular reactivity by the pattern of response to progressive hypercapnia. *Hum Brain Mapp*. 2017. [Epub ahead of print].
14. Liu P, Welch BG, Li Y, et al. Multiparametric imaging of brain hemodynamics and function using gas-inhalation mri. *NeuroImage*. 2017;146:715-723.
15. Uchino H, Kuroda S, Hirata K, Shiga T, Houkin K, Tamaki N. Predictors and clinical features of postoperative hyperperfusion after surgical revascularization for moyamoya disease: a serial single photon emission ct/positron emission tomography study. *Stroke*. 2012;43(10):2610-2616.
16. Vorstrup S, Brun B, Lassen NA. Evaluation of the cerebral vasodilatory capacity by the acetazolamide test before ec-ic bypass surgery in patients with occlusion of the internal carotid artery. *Stroke*. 1986;17(6):1291-1298.
17. Stokely EM, Sveinsdottir E, Lassen NA, Rommer P. A single photon dynamic computer assisted tomograph (dcat) for imaging brain function in multiple cross sections. *J Comput Assist Tomogr*. 1980;4(2):230-240.
18. Yun TJ, Paeng JC, Sohn CH, et al. Monitoring cerebrovascular reactivity through the use of arterial spin labeling in patients with moyamoya disease. *Radiology*. 2016;278(1):205-213.
19. Bulte DP, Kelly M, Germuska M, et al. Quantitative measurement of cerebral physiology using respiratory-calibrated mri. *NeuroImage*. 2012;60(1):582-591.
20. Tancredi FB, Lajoie I, Hoge RD. Test-retest reliability of cerebral blood flow and blood oxygenation level-dependent responses to hypercapnia and hyperoxia using dual-echo pseudo-continuous arterial spin labeling and step changes in the fractional composition of inspired gases. *J Magn Reson Imaging*. 2015;42(4):1144-1157.
21. Su P, Mao D, Liu P, et al. Multiparametric estimation of brain hemodynamics with mr fingerprinting asl. *Magn Reson Med*. 2017;78(5):1812-1823.
22. Federau C, Christensen S, Zun Z, et al. Cerebral blood flow, transit time, and apparent diffusion coefficient in moyamoya disease before and after acetazolamide. *Neuroradiology*. 2017;59(1):5-12.
23. Roach BA, Donahue MJ, Davis LT, et al. Interrogating the functional correlates of collateralization in patients with intracranial stenosis using multimodal hemodynamic imaging. *AJNR-Am J Neuroradiol*. 2016;37(6):1132-1138.
24. Donahue MJ, Strother MK, Lindsey KP, Hocke LM, Tong Y, Frederick BD. Time delay processing of hypercapnic fmri allows quantitative parameterization of cerebrovascular reactivity and blood flow delays. *J Cereb Blood Flow Metab*. 2016;36(10):1767-1779.
25. Donahue MJ, Dethrage LM, Faraco CC, et al. Routine clinical evaluation of cerebrovascular reserve capacity using carbogen in patients with intracranial stenosis. *Stroke*. 2014;45(8):2335-2341.
26. Faraco CC, Strother MK, Siero JC, et al. The cumulative influence of hyperoxia and hypercapnia on blood oxygenation and R 2 ∗. *J Cereb Blood Flow Metab*. 2015;35(12):2032-2042.
27. Mugikura S, Takahashi S, Higano S, Shirane R, Sakurai Y, Yamada S. Predominant involvement of ipsilateral anterior and posterior circulations in moyamoya disease. *Stroke*. 2002;33(6):1497-1500.
28. Allen LM, Hasso AN, Handwerker J, Farid H. Sequence-specific mr imaging findings that are useful in dating ischemic stroke. *RadioGraphics*. 2012;32(5):1285-1297; discussion 1297-1289.
29. Smith SM, Jenkinson M, Woolrich MW, et al. Advances in functional and structural mr image analysis and implementation as fsl. *NeuroImage*. 2004;23(suppl 1):S208-S219.
30. Jenkinson M, Smith S. A global optimisation method for robust affine registration of brain images. *Med Image Anal*. 2001;5(2):143-156.
31. Pexman JH, Barber PA, Hill MD, et al. Use of the alberta stroke program early ct score (aspects) for assessing ct scans in patients with acute stroke. *AJNR Am J Neuroradiol*. 2001;22(8):1534-1542.
32. Han JS, Abou-Hamden A, Mandell DM, et al. Impact of extracranial-intracranial bypass on cerebrovascular reactivity and clinical outcome in patients with symptomatic moyamoya vasculopathy. *Stroke*. 2011;42(11):3047-3054.
33. Mandell DM, Han JS, Poublanc J, et al. Quantitative measurement of cerebrovascular reactivity by blood oxygen level-dependent mr imaging in patients with intracranial stenosis: preoperative cerebrovascular reactivity predicts the effect of extracranial-intracranial bypass surgery. *Am J Neuroradiol*. 2011;32(4):721-727.
34. Fushimi Y, Okada T, Takagi Y, et al. Voxel based analysis of surgical revascularization for moyamoya disease: pre- and postoperative spect studies. *PLoS One*. 2016;11(2):e0148925.
35. Mukawa M, Nariai T, Inaji M, et al. First autopsy analysis of a neovascularized arterial network induced by indirect bypass surgery for moyamoya disease: Case report. *J Neurosurg*. 2016;124:1211-1214.
36. Desai AA, Strother MK, Faraco CC, et al. The contribution of common surgically implanted hardware to functional mr imaging artifacts. *Am J Neuroradiol*. 2015;36(11):2068-2073.
37. Sugino T, Mikami T, Miyata K, Suzuki K, Houkin K, Mikuni N. Arterial spin-labeling magnetic resonance imaging after revascularization of moyamoya disease. *J Stroke Cereb Dis*. 2013;22:811-816.
38. Lu H, Clingman C, Golay X, van Zijl PC. Determining the longitudinal relaxation time (t1) of blood at 3.0 tesla. *Magn Reson Med*. 2004;52:679-682.
39. van Osch MJ, Teeuwisse WM, van Walderveen MA, Hendrikse J, Kies DA, van Buchem MA. Can arterial spin labeling detect white matter perfusion signal? *Mag. Reson Med*. 2009;62:165-173.

Supplemental digital content *is available for this article at www.neurosurgery-online.com.*

Supplemental Digital Content 1. Figure. Regions of interest used for determination of vascular compliance measures. A T_1-weighted atlas is shown in **A**. Middle cerebral artery (MCA) and posterior cerebral artery territory were determined by including all tissue in the area of corresponding MCA Alberta Stroke Programme early CT score (ASPECTS) regions. Axial slices with overlaid territory map for the MCA and posterior cerebral artery territory are shown in (**B**; right MCA in blue, left MCA in red) and **C**, respectively. MCA territories of the operative hemispheres were analysis for mean values pre- and post-revascularization. CVR_{RAW} and CVR_{MAX} values were normalized by the posterior cerebral artery territory.

Supplemental Digital Content 2. Figure. Comparison of vascular compliance measures between carbogen (5% CO_2 / 95% O_2) and hypercapnic normoxia (5% CO_2 / 95% air) in controls. Cerebrovascular reactivity measures (CVR_{RAW} and

CVR_{MAX}) in addition to CVR_{DELAY} measures were evaluated in healthy control subjects (n = 9) in the left middle cerebral artery (MCA) territory (diamond), right MCA territory (triangle), and posterior circulation (circle). Region-of-interest correlations were evaluated between the vascular stimuli; to allow for comparison across all voxels, no normalization by values in posterior circulation was performed to understand absolute relationships. A significant correlation was observed between carbogen and hypercapnic normoxia in CVR_{RAW} (**A**, $\rho = 0.53$, $P = .0024$), CVR_{MAX} (**B**, $\rho = 0.45$, $P = .0097$), and CVR_{DELAY} (**C**, $\rho = 0.42$, $P = .014$). Panel **D** demonstrates a nonsignificant difference between CVR_{DELAY} values between carbogen and hypercapnic normoxia stimulus. As expected, CVR_{DELAY} values in moyamoya participants were significantly elevated compared to controls.

Supplemental Digital Content 3. Figure. Additional axial slices from patients shown in Figure 4. Panel **A** shows a patient with >1/3 MCA territory revascularization, and panel **B** shows a patient with <1/3 MCA territory revascularization.

Supplemental Digital Content 4. Figure. Correlation of CVR compliance measures and BOLD signal change in middle cerebral artery territory of operative hemispheres in participants with moyamoya.Relative BOLD signal change ($\Delta S/S_0$) is defined as the mean difference in the signal during the final 90 s of each stimulus block (total stimulus block duration = 180 s) and baseline block, divided by the mean signal during the final 90 s of the baseline block. Unnormalized (eg, prior to normalization by posterior cerebral artery flow territory) z-statistic values are reported for CVR_{RAW} and $CVR_{MAX,}$ and are plotted against $\Delta S/S_0$ and shown in panels **A** and **B**, respectively. Normalized z-statistic values of $rCVR_{RAW}$ and $rCVR_{MAX}$ are plotted against normalized $\Delta S/S_{0,}$ and shown in panels **C** and **D**, respectively. CVR_{RAW} and CVR_{MAX} are significantly correlated with $\Delta S/S_0$ ($P = .002$, $P < .001$, respectively). When evaluating normalized measures, both $rCVR_{RAW}$ and $rCVR_{MAX}$ are significantly correlated on average with normalized $\Delta S/S_0$ ($P = .014$, $P = .014$, respectively).

Supplemental Digital Content 5. Figure. Receiver operating characteristic (ROC) curve analysis of vascular compliance measures. Changes in each vascular compliance measure were calculated, and hemispheres with >1/3 to <1/3 MCA territory revascularization were compared to perform ROC analysis. The area under the ROC was >0.70 for $rCVR_{RAW,}$ and CVR_{DELAY} indicating that changes in these compliance measures may be acceptable for separating robust from minimal revascularization. However, ROC interpretation is limited by the sample size of the <1/3 MCA revascularization (n = 5).